1 INTRODUCTION

Hard Turning is an established process in industry for the finish machining of a wide range of hardened steel work pieces. It is typically used for components, where requirements for accuracy and surface finish are not too demanding. In high- and ultra-precision applications grinding is still the commonly used manufacturing process. This is sometimes complemented by dedicated finishing processes when even better surface finishes are required.

In comparison to grinding, hard turning can offer significant advantages, namely that it is a far more flexible manufacturing method. Hard turning - often used as a dry cutting process - has also great ecological advantages. In spite of the obvious advantages hard turning is rarely used for the manufacture of precision and ultra-precision work pieces.

One of the major obstacle that must be overcome before hard turning can be used as an ultra-precision manufacturing process is that the surface finishes achieved by hard turning cannot yet rival those achieved by ultra-precision grinding machines.

Increasing awareness of the potential benefits of hard turning as an ultra precision manufacturing process has lead to great interest in improving the process capability so that surfaces with optical quality can be manufactured by hard turning.

The wider aim of this thesis is to establish the feasibility of hard turning surfaces to a roughness of $R_a < 0.01$ µm. If suitable process conditions were to be found this would potentially revolutionise the finish machining of hard steel components in industries as diverse as automotive and aerospace as well as the manufacture of optical components and moulds.

2 LITERATURE REVIEW

2.1 The hard turning process

2.1.1 The principle of hard turning

The set-up for hard turning differs little from the set-up of other turning processes. The work piece carries out a rotation about its longitudinal axis. As a result of this the work piece surface moves relative to the cutting tool at the cutting speed v_c. Superimposed on the cutting speed is a second, orthogonal motion, which can be carried out by either the cutting tool or the work piece. This motion is the feed motion f and causes a relative translation of the cutting tool over the work piece surface along the desired cutting path. The principle of hard turning is shown in Figure 1.

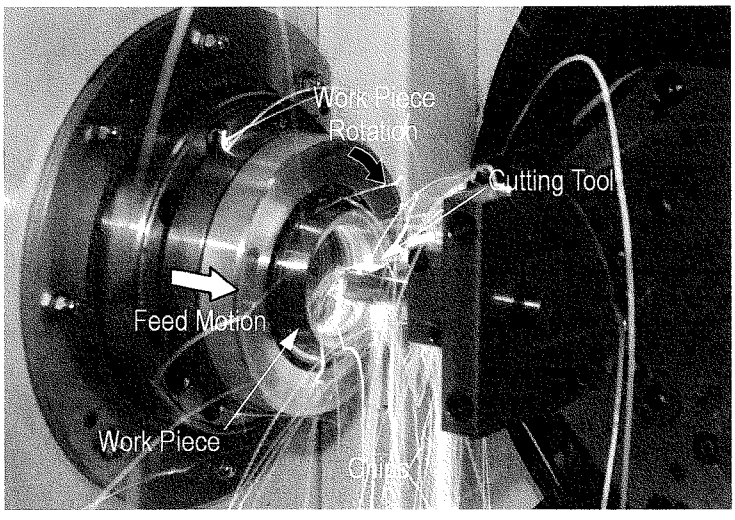

Figure 1: Principle of Hard Turning

Having stated that the set-up of hard turning is similar to that in soft turning, it must be pointed out that the boundary conditions are distinctly different. First of all the work pieces machined by hard turning are made from hard steel. Hardness figures range from approximately 40 to 70 *HRc*. In terms of machining parameters hard turning is particularly characterised by low feeds (f) and small depths of cut (a_p). There are other processes, in particular the machining of some cast irons, which are also sometimes referred to as "hard turning". These are not considered in this thesis.

Also typical for hard turning – being a dry cutting process – is the high heat generation. This is apparent by the often brightly glowing chips flowing off the work piece, which has been examined in more detail in [1]. Using finite element models and experimental data, temperatures in hard turning were assessed and a good correlation between models and experiments found. According to this paper the maximum temperature in hard turning is reached at the chip-tool interface and can reach as much as 729°C. There are two primary sources for this high temperature: The deformation of the chip in the primary shear zone and friction in the chip-tool interface.

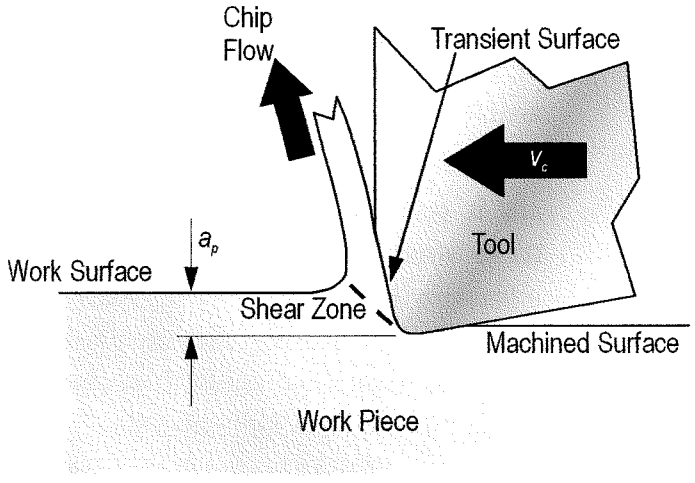

Figure 2: Chip formation in hard turning

The temperature is affected by cutting speed as well as the thermal conductivity of the cutting material. Higher cutting speeds cause a greater energy input per unit time and therefore increase cutting temperatures, while higher thermal conductivity of the cutting tool allows more energy to be dissipated from the chip-tool interface and thus reduced temperatures.

Two theories exist on the mechanisms involved in hard turning - thermodynamic theory and hydrostatic theory. The older, more established theory is the thermodynamic one. It is argued that hard steel can only be machined if it is softened by the process heat [2]. This is commonly referred to as "self induced hot machining". The theory says that a zone of high temperature travels in front of the cutting tool through the work piece much like a bow wave. This causes a local softening of the hard steel. The softening leads to a reduction in cutting force and allows a ductile deformation in the shear zone without brittle fracture of either chip or the base material.

Brandt [3] makes the criticism that, if the thermodynamic theory is applied, the cutting behaviour should be strongly dependent on the thermal conductivity of both work piece and cutting material. In his work he seems to have found very little evidence of this effect. A different theory was therefore proposed, arguing that under sufficient compressive stress brittle materials can be deformed plastically.

The cutting conditions in hard turning are such that very high compressive stresses are achieved in the cutting zone. Cutting tools used for hard turning typically have a negative rake angle on the major first face, which carries out most of the cutting action. They also have a cutting edge radius which is often only two to three times smaller than the depth of cut and leads to what are effectively even more strongly negative face angles.

These strongly negative angles create very high stresses in the work piece and in particular in the region of the primary shear zone. It is argued that these stresses are high enough to allow a plastic deformation of the otherwise brittle work piece material, similarly to the effect that even materials like marble can be plastically deformed if subjected to high enough compressive stress. It is argued that the high temperatures in hard turning are a by product rather than a pre-requisite for hard turning.

The hydrostatic theory is consistent with Mohr's shear stress hypothesis [4]. It is further supported by [5], where a positive effect on the hard turning process was achieved by high-pressure water jet cooling of the chip-tool interface. If the process heat was as important as postulated by the thermodynamic theory then the water jet cooling should not lead to a reduction in cutting force.

Having stated this it cannot be ruled out that there is no thermodynamic effect in hard turning or indeed in which proportion it contributes to the functioning of the cutting process.

2.1.2 Surface roughness

Boundaries of solid bodies are formed by their surfaces. In engineering terms these boundaries are typically described as geometrically perfect surfaces in drawings (or computer models), referred to as the geometrical surface. Manufactured components always show deviations from the geometrical surface. Surface roughness is one aspect of the deviations from the geometrical surface. Size, form and waviness are other aspects of the deviation.

In order to obtain surface roughness a profile is determined by measuring deviations normal to the geometric surfaces. For practical purposes long-wave deviations such as form error and waviness are eliminated from the measured profile prior to calculation of the surface finish.

In cases where a surface has a regular pattern or lay the profile is typically recorded across the lay, so that the amplitude of the profile is at its maximum.

The main surface finish parameters used in the ongoing work will be R_t and R_a. Their definition and mathematical derivation is explained below (Figure 3). Definitions for other parameters can be found in [6], [7], [8].

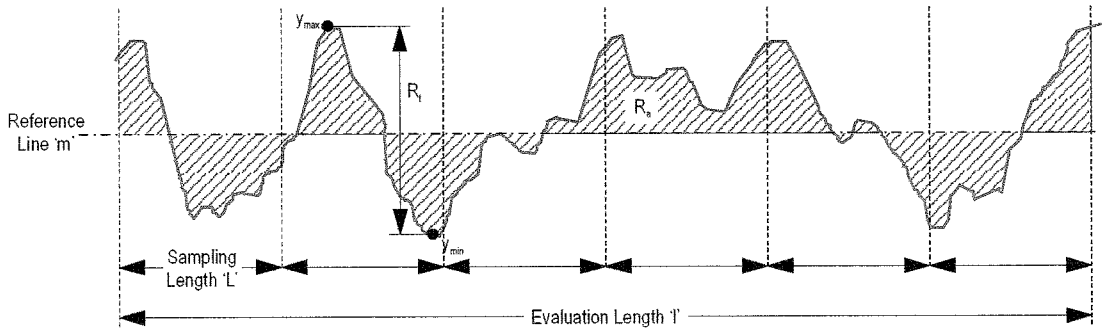

Figure 3: Surface Roughness

The reference line m is used as a datum for the calculation of a number of surface finish parameters. It is calculated as a least-square fit to the points recorded over the evaluation length. The total area above the reference line and enclosed by the recorded trace is therefore equal to the area enclosed between the reference line and the trace below it.

R_t (derived from the German Rauhtiefe, roughness depth) measures the vertical distance between the highest (y_{max}) and the lowest point (y_{min}) in the evaluation length.

Equation 1:

$$R_t = y_{\max} - y_{\min}$$

R_a (for roughness average) is the average deviation of measured values from the reference line. The mathematical definition is given in Equation 2.

Equation 2:

$$R_a = \frac{1}{l}\int_0^l |y|\,dx$$

If the profile is recorded as a series of 'n' discrete points (y_1 to y_n) around the reference line taken at constant sampling intervals, R_a can be approximated as:

Equation 3:

$$R_a \approx \frac{|y_1|+|y_2|+|y_3|+\ldots+|y_n|}{n}$$

2.1.3 Surface generation

In turning the work piece revolves under the moving cutting tool, which causes the tool to follow a helical path over the work surface. With each revolution of the work piece an imprint of the cutting tool's profile is left on the machined surface. Each imprint is separated from the next by the distance of the feed *f*.

As a result of the feed motion a continuous chip is removed from the work piece. This chip has a non-uniform profile in its undeformed shape (as illustrated in Figure 4) and is distorted further in the shear zone. The undeformed chip thickness changes depending on the tool cutting edge angle κ_{re} (see Figure 4). With decreasing cutting edge angle the undeformed chip thickness *h* also decreases until it reaches zero thickness at the intersection between tool profile and previously machined work piece surface.

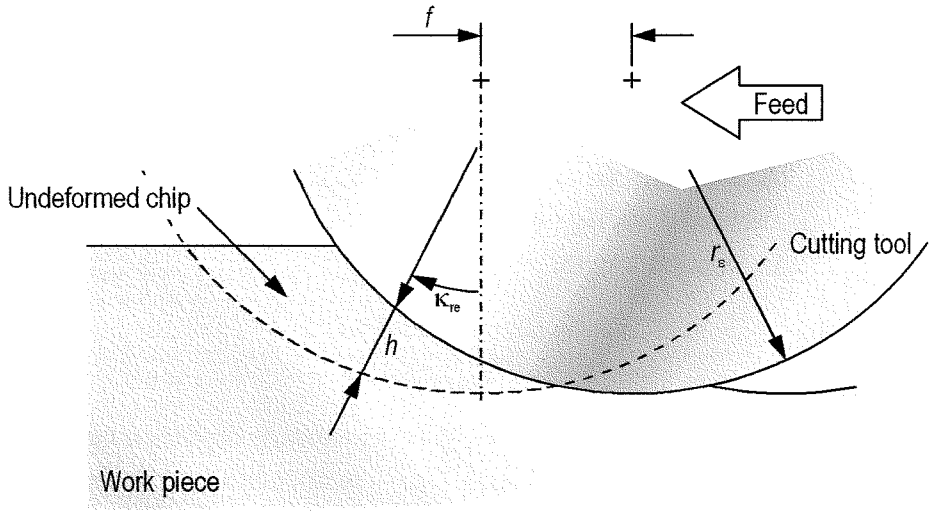

Figure 4: Dimensions and shape of the undeformed chip

With a known tool profile - typically a radius - it is possible to calculate the machined surface profile. A frequently used assessment parameter is the surface peak-to-valley height R_t. This is illustrated in Figure 5.

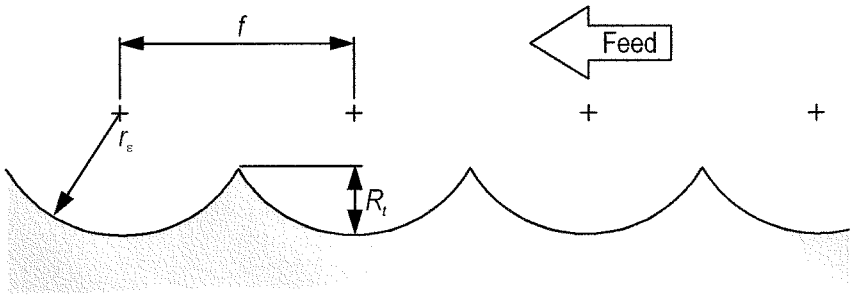

Figure 5: Surface roughness generation in turning

With a given corner radius and feed the peak-to-valley height of the machined surface can be calculated as:

Equation 4:

$$R_t = r_\varepsilon - \sqrt{r_\varepsilon^2 - \frac{f^2}{4}}$$

or

$$R_t \approx \frac{f^2}{8 \cdot r_\varepsilon}$$

Equation 4 only applies under the conditions that the tool profile is a perfect circular arc and an exact imprint of the tool is left on the work piece surface. In spite of this Equation 4 works well for many turning applications at high feed rates [9]. A formula which is claimed to give more accurate results at low feed rates is given by Brammerz [10]. He argued that the cutting can only take place if a sufficient undeformed chip thickness is maintained. As the cutting edge angle κ_{re} is reduced the undeformed chip thickness reduces in turn and at a certain threshold value becomes smaller than h_{min}. As a result no cutting takes place in a region on the cutting tool where κ_{re} is small.

If the undeformed chip thickness is smaller than this minimum value the cutting tool will not remove a chip from the work piece; instead the tool will slide over the work piece surface, while both the work piece and the cutting tool deform to allow the work piece material to pass under the tool.

In [10] it is assumed that this deformation of tool and work piece in the area of the chip root is purely elastic and fully reconstitutes itself to its original shape once the contact conditions change.

Equation 5 takes into account the effect of the minimum undeformed chip thickness. Note that Equation 4 and Equation 5 give very similar values for R_t, if $f >> h_{min}$.

Equation 5:

$$R_t = r_\varepsilon \cdot \left[1 - \sqrt{1 - \frac{f^2 + 2 \cdot r_\varepsilon \cdot h_{\min} - h_{\min}^2}{2 \cdot r_\varepsilon \cdot f}} \right]$$

or

$$R_t \approx \frac{f^2}{8 \cdot r_\varepsilon} + \frac{h_{\min}}{2} \cdot \left(1 + \frac{r_\varepsilon \cdot h_{\min}}{f^2} \right)$$

The difficulty with Equation 5 is in determining the minimum undeformed chip thickness h_{min}. Normally this is done by using L'Vov's work [11]. L'Vov examined the forces exerted on the chip by the cutting edge according to the principles of classical mechanics.

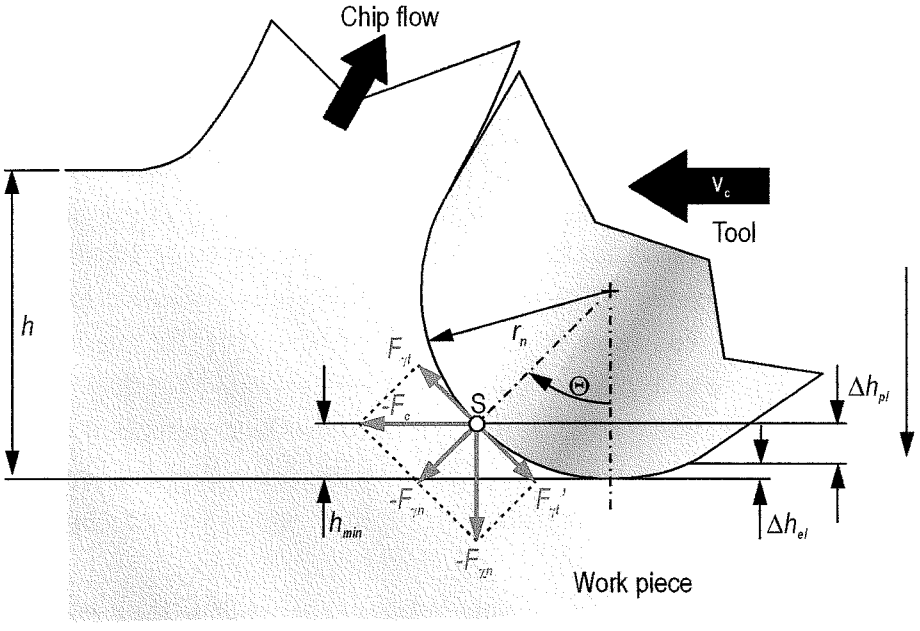

Figure 6: Determination of the stagnation point according to L'Vov[1]

[1] L'Vov used different abbreviations and symbols in his work. These have been changed to comply with [65], [66]

L'Vov argued that on a point on the chip-tool-interface, the force acting on the chip in this point is $-F_{\gamma n}$. According to classical mechanics this force can be split into the orthogonal components $-F_c$ and $-F_{\chi n}$. These in turn can be used to calculate the tangential forces acting on the chip in a particular point ($F_{\gamma t}$ and $F_{\gamma t}'$). In the stagnation point S the tangential forces are equal. Any material above the stagnation point is exposed to a larger upward force and will therefore move upward into the chip. Any material below the stagnation point is exposed to a larger downward force and will be forced into the gap between the tool and the work piece.

Contrary to the assumption in [10] L'Vov highlights that this material can undergo both elastic (Δh_{el}) and plastic (Δh_{pl}) deformation, of which only the elastic deformation reconstitutes itself once the material has passed the cutting tool.

If L'Vov's argument is accurate then the stagnation point always occurs at $\Theta = 45°$. It follows that:

Equation 6:

$$h_{\min} = r_n \cdot (1 - \cos\Theta)$$
$$\text{with } \Theta = 45°$$
$$h_{\min} = 0.293 \cdot r_n$$

Recent work however suggests that the classical mechanics approach is not an accurate way of determining the stagnation point angle Θ. Experimental work was carried out by Schmidt [12] using a range of hard turning tools with different cutting edge radii. According to these results the stagnation point angle is $\Theta \approx 25°$.

Equation 7:

$$h_{\min} = r_n \cdot (1 - \cos\Theta)$$
$$\text{with } \Theta = 25°$$
$$h_{\min} = 0.09369 \cdot r_n$$

With good approximation it is possible to use the following relationship:

Equation 8:

$$h_{\min} \approx 0.1 \cdot r_n$$

Interestingly computer simulation of diamond turning [13] has led to the same conclusion as Equation 8.

2.1.4 Surface integrity

When work pieces are machined not only is the geometry of the surface affected in macroscopic and microscopic terms. The machining process induces a number of changes in the surface layers of a work piece. The most important characteristics affected in hard turning are:

Metallurgical changes are generally accepted to be the result of thermal effects during the machining process. Factors which affect heat transfer into the work piece surface consequently affect the degree and type of metallurgical change.

A detailed assessment of the generation of *white layers* is made in [3]. A strong link is made between the wear state of the cutting tool and the formation of white layers. The mechanism involved is described as follows:

Hardened steel typically consists of a martensitic structure. Temperatures generated during hard turning typically reach 700-800°C [14] although higher temperatures have been reported [15], which is above the work piece's austenite temperature. However work pieces machined with unworn tools show no discernible changes near the machined surface when compared to the bulk material. The heat flux into the machined surface is insufficient for white layers to form. Instead most of the heat is removed with the chip.

As the cutting tool wears, a wear flat is generated on the face of the tool which rubs over the already machined surface. Heat generated here cannot be removed with the chip and therefore directly impacts on the work piece surface. The use of worn tools leads to the generation of an austenite rich surface layer, whose thickness is dependent on the degree of tool wear. These austenitic layers appear white in etched samples and are therefore referred to as "white layers". A threshold value for tool wear in precision hard turning is given as a wear mark width of typically V_B=150µm, above which white layers are generated.

The austenitic white layers generated by hard turning have a less detrimental effect on the work piece and must not be confused with the amorphous white layers generated by other machining processes such as grinding, which severely degrade work piece quality [16]. In some cases it is even argued that the white layers can be tribologically advantageous [17].

Also affected by the heat transfer into the bulk material during the hard turning process is the *surface hardness* of the work piece. A range of factors influence the work piece hardness. One of the main factors obviously is the composition and heat treatment condition of the work piece. In addition cutting parameters also affect hardness. Bongardt and Werner [18] report on their findings on the effects of cutting parameters on surface hardness and hardness depth. A subset of their results is shown in Figure 7. Note that these hardnesses were recorded on the tip of the turning cusps, where very high hardness values dominate. Measuring hardnesses in the bottom of the feed marks led to a reduction of up to 25%.

When cutting with emulsion coolant, increases in feed rate led to a decrease in peak surface hardness, but to an increase in hardness depth. The same trend in hardness depth is seen for increased cutting speeds, even though there does not seem to be a clear trend in peak surface hardness. Both effects it is claimed are due to the increased energy transmitted into the work piece surface when increasing feed or cutting speed. The strong quenching effect of the coolant leads to the reported high hardnesses.

In dry cutting the trend is even more evident. Higher feed rates not only led to higher hardness depths they also led to higher peak hardnesses. The reduced depth of cut and the absence of the quenching effect of the coolant lead to lower overall observed hardnesses.

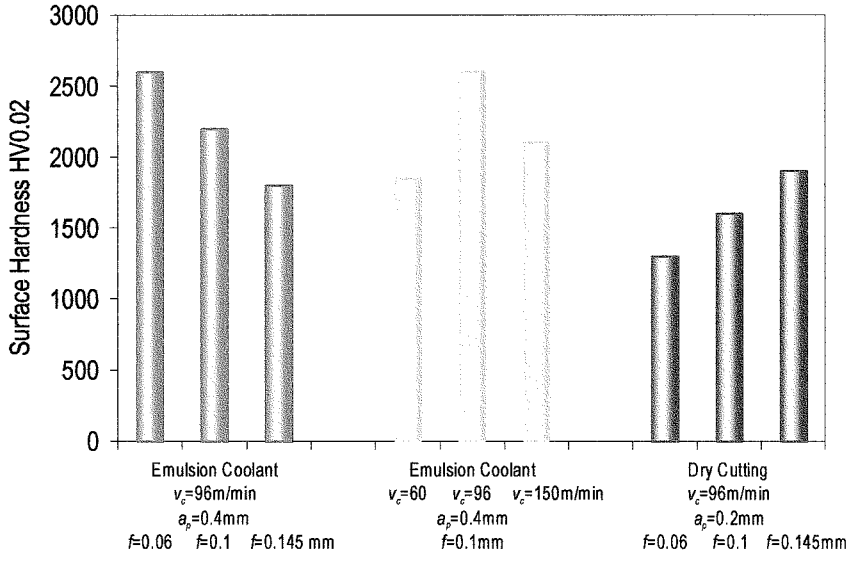

Figure 7: Approximate surface hardness values (HV0.02) depending on process conditions given by Bongardt [18]

Residual Stress: The deformation of the work piece material during the machining process results in stresses in the work piece surface. Typically these stresses are large in magnitude near the surface and decrease with distance from the machined surface. A qualitative residual stress profile is shown in Figure 8. Profiles like this have been reported by a number of researchers [2], [19], [20], [3], [21], to name only a few.

Common to all of the above publications, is the fact that the magnitudes as well as stress profiles greatly depend on the process condition. In [19] the effect of work piece hardness on residual stress under otherwise constant machining conditions is reported. AISI4340 steel in hardnesses ranging from *HRc* 29 to *HRc* 56 were tested. Measured in the cutting directions the resulting trend was that softer steel exhibited tensile residual stress on the work piece surface with only low compressive stress at low penetration depths. As harder and harder work piece material was used, the initial residual stress became strongly compressive and showed higher penetration depth.

Brandt [3] on the other hand assessed residual stress as a function of tool wear. Comparing residual stress in work pieces machined with cutting tools with different wear mark widths, sharp cutting tools produced compressive residual stress on the work piece surface, but low penetration. In contrast increased tool wear lead to larger tensile residual stress and higher penetration of stresses, both tensile and compressive, into the work piece.

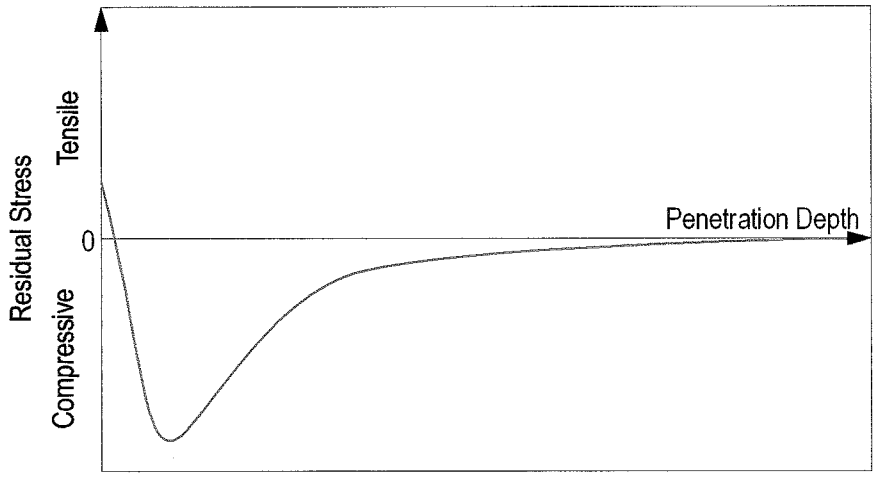

Figure 8: Typical Residual Stress Profile in hard turning

The importance of residual stresses in machining is their effect on component life under mechanical loading. Compressive residual stresses can give a significantly improved component life over those with tensile residual stresses [22], [23], [24], [16], [25].

The causes for residual stresses in turning are mainly due to two sources: mechanical deformation of the chip in the shear zone and thermal effects from cutting and friction between tool and machined surface [26]. Generally it is assumed that the chip removal i.e. the mechanical cutting action in hard turning causes predominately compressive stresses of higher penetration, while the thermally induced residual stresses are tensile and do not penetrate deeply into the work piece. The superposition of the two stress fields give the characteristic profile shown in Figure 8.

There are differing reports on the effect of various cutting parameters on residual stress. The interaction between work piece material, cutting parameters (depth of cut, feed, cutting speed), cutting tool material, cutting tool geometry (corner radius, face angle, cutting edge radius) and machine tool related influences seem to be too complex to come to generalised conclusions about their effects on residual stress.

2.1.5 Cutting tools

The cutting tools used for hard turning have to withstand very high pressures and elevated temperatures. Although other materials are used, cutting tools offered for finish hard turning are made almost exclusively from polycrystalline cubic boron nitride (CBN) [27], [28], [29]. CBN is one of the hardest known materials and retains its hardness at high temperatures. It also remains chemically stable at elevated temperatures. These properties make CBN a material well suited to the hard turning process. [2], [30].

In these hard turning tools the cubic boron nitride (CBN) is embedded in a ceramic binder phase. In addition to their mechanical properties the binders act as thermal insulators. PCBN is an excellent heat conductor and without the presence of the binder a significant amount of heat would be conducted away from the cutting zone. Although there are different theories about the cutting mechanism and the importance of maintaining elevated temperatures as outlined in Section 2.1.1, excessive heat flux into the cutting tool can lead to failure of the braze, which holds the CBN insert in place.

CBN Grade	CBN Content	CBN Size	Binder	Tensile Strength [N/mm²]	Thermal Conductivity [W/m/K] (at 20°C)	Coating
BN600	High	Medium	*unknown*	800	*unknown*	none
BNX10	Low	Medium	TiC	800-900	*unknown*	none
BNX20	Medium	Medium	TiN	950-1100	*unknown*	none
BNX25	Low	Ultra Fine	Carbide	*unknown*	*unknown*	none
BNC80	*unknown*	*unknown*	*unknown*	*unknown*	*unknown*	TiN
CBN100	50%	2µm	TiC	*unknown*	29	none
CBN100P	50%	2µm	TiC	*unknown*	*unknown*	Ti(C,N) + (Ti, Al) N + TiN flash
CBN150	45%	<1µm	TiN	*unknown*	34	none
CBN300	90%	22µm[2]	Al-Ceramic	*unknown*	138	none

Table 1: CBN grades used for turning of hard steel

Table 1 lists the CBN grades used in the course of this work. CBN tools from two different manufacturers were used, covering the widest available range of their respective products in terms of grain size and CBN content. CBN grain size ranged from an average of 22µm down to less than 1µm; with CBN content ranging from 45% to 90%.

Unfortunately there is no published numerical data available for the first five listed CBN grades.

Also included are two different coated CBN grades. BNC80 is coated with what is described as a TiN coating, the other is a CBN100 grade with a multi-layer coating.

[2] CBN300 is a multimodal CBN incorporating a range of grain sizes with an average size of 22µm.

2.1.5.1 Tool wear

Wear of CBN cutting tools in continuous hard turning is caused by a number of different mechanisms. Abrasion and small scale attrition of the cutting edge are thought to cause the majority of the wear [31], [32].

It has been shown that the microstructure and chemical composition of the work piece have a significant impact on abrasive wear in hard turning. In particular it is possible to correlate tool wear rate with the size of carbides contained in the work piece material. But also the size of the grain structure of the work piece material affect tool wear. It is reported that the use of fine grain powder metallurgical steel leads to a considerable reduction in tool wear [33].

There is also an element of chemical interaction between the work piece and the cutting tool. The formation of a liquid phase in the cutting zone is reported in [15]. The constituents of that liquid phase are reaction products of work piece and cutting tool material with a lower melting point than either of the two individual materials. The chemical wear phenomena are strongly dependent on cutting speed. The increase in cutting zone temperature associated with high cutting speeds can lead to considerable chemical tool wear. Despite the fact that chemical wear occurs, the products of the chemical reaction can contribute to an overall reduction in tool wear by forming a protective coating on the cutting tool. This coating reduces friction between tool and work piece or chip surface and leads to a reduction in abrasive wear.

More evidence of the protective nature of reaction by-products is given in [34]. Here the wear of CBN tools is compared for the machining of grey iron and compacted graphite iron (CGI). It is observed that the tool life in machining CGI is reduced in comparison to grey iron, in particular at high feed rates. Examination of the used cutting tools reveals a protective Manganese-Sulphur layer on the cutting tools used to machine grey iron. CGI contains only very small quantities of Sulphur, not enough to form a MnS layer on the cutting edge. The severe wear effect of CBN tools is also described in [35].

Having described the mechanisms involved in hard turning, it is also important to assess the way in which wear manifests itself on the cutting tool. Wear patterns in hard turning are normally assessed in two planes parallel to the tool back plane and the tool reference plane.

In the tool back plane (Figure 9) wear occurs in distinctive zones [12]. Wear on tool face, cutting edge and flank are bounded by areas where no tribological contact takes place and no wear is visible. The majority of the wear takes place on the tool face and flank, although - due to the changing geometry of the adjacent faces - a certain amount of retraction of the cutting edge is unavoidable.

Wear on the face of the tool is caused by the chip flowing over the face before losing contact with the face. The extreme pressures and temperatures in this area cause tool material to be worn away. In particular at high depths of cut and high feed rates wear in form of a crater occurs underneath the chip. Crater wear changes the effective face angle and can lead to a change cutting behaviour. Excessive crater wear hollows out the area of the tool immediately behind the cutting edge. As a result a sudden collapse of the cutting edge can take place. This leads to a severe degradation of cutting performance normally spells the end of life for this particular cutting tool.

The flank wear takes on the shape of a flattened off area on the cutting tool. The width of the flank wear, referred to as the wear mark width V_B, is a good indicator for the state of the cutting tool [3]. An increase in wear mark width leads to increased friction between cutting tool and work piece. As a consequence a higher push-off force and more heat is created in the cutting process. As the heat generated by rubbing cannot be removed in the chip it has a direct impact on the work piece. It has been shown that a wear mark width of up to 100-150µm does not lead to work piece damage. Once a wear mark width of 150µm is exceeded the increased process heat leads to significant white layer formation on the work piece surface [3].

Wear seen in the tool reference plane (Figure 10) is characterised by a wear 'flat' which is the result of flank wear described above. The wear flat is seldom perfectly flat, but leads to an increase in effective cutting tool radius (r_ε). The change in cutting edge shape and topography then impacts on the achievable surface finish [36], [32].

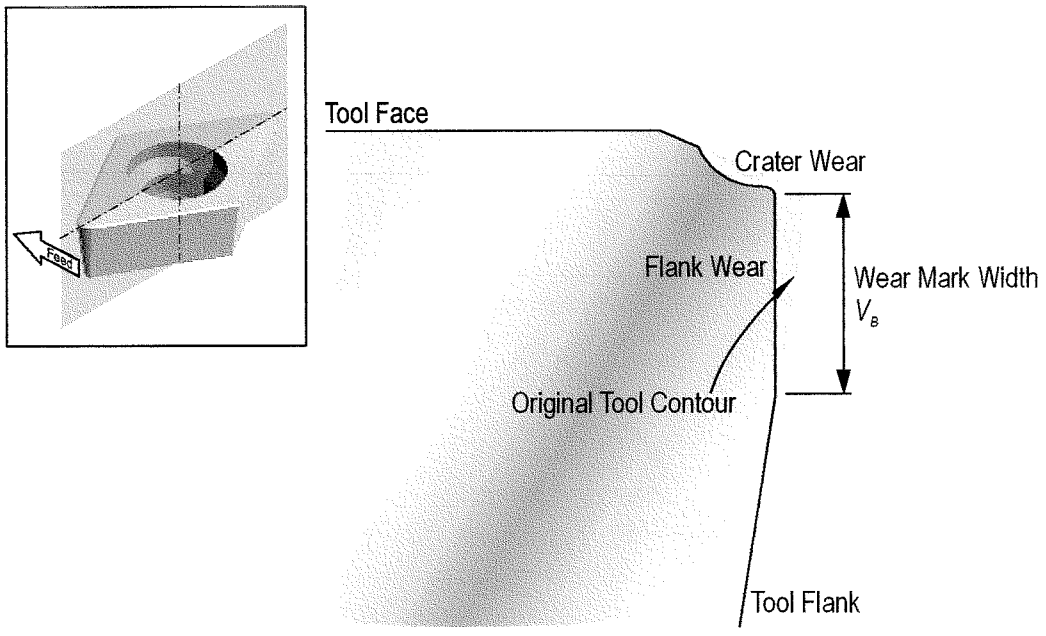

Figure 9: Tool wear in section parallel to the Tool Back Plane

A common phenomenon when examining tool wear in the tool reference place is the occurrence of notch wear [36]. The notch wear always seems to occur on the trailing edge of the cutting tool and correlates in position with the area of low undeformed chip thickness predicted in [10]. The high pressures in the region of the minimum undeformed chip thickness cause plastic deformation of the cutting edge, causing the notch to form. Subsequent abrasive wear on the length of the engaged cutting edge causes the cutting edge to retreat. Further abrasive wear on the leading edge of the cutting tool leads to a distinct change in shape of the cutting tool where the achievable surface finish mainly depends on the angle of the newly created trailing edge.

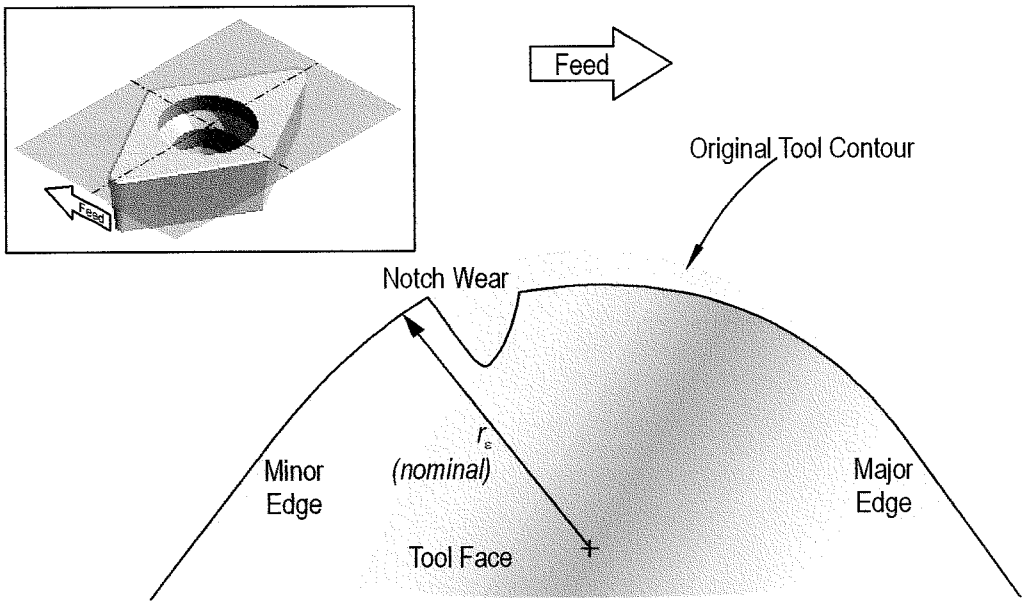

Figure 10: Tool wear in section parallel to the Tool Reference Plane P_r

2.1.6 Modelling of the hard turning process

When assessing the modelling of machining processes in general and hard turning in particular two fundamentally different types of models are encountered. The majority of the published work describes models of cutting processes in the tool back plane (Figure 9), similar to the illustration shown in Figure 2. The reason for this is that despite the fact that these models are two dimensional a lot of relevant data about the cutting process can be derived from this model and they are instrumental in understanding chip formation.

Early models such as those described in [37], [38] attempt to explain chip formation and derived quantities such as cutting forces in analytical models. The analytical models require some degree of simplification and achieved "satisfactory agreement with experiment". More recent and complex analytical models, for example [39], are specifically designed to model hard cutting and can explain with good results the chip shape obtained in hard turning.

It has been attempted to create more comprehensive models of hard turning by the finite element method. These models can potentially simulate the details of chip formation and arising stress or strain both in the chip as well as the work piece. In addition cutting related forces and temperatures can be modelled [40], [1], [14]. While the finite element models are an improvement over the analytical models in that they can include more parameters it is generally conceded that they still have some inherent inaccuracies. This is mainly due to the fact that these models are two dimensional and do not take into account the varying undeformed chip thickness encountered in practice. A 3D finite element model aimed at refining the simulation of temperatures, residual stress and chip flow is described in [41]. While this model correlates well with experimental data, it also shows the current limits of the method. With element sizes in the order of 0.1mm the model is not capable of resolving the finer and potentially important details of the hard turning process such as effects of the cutting edge radius and the minimum undeformed chip thickness which are at least one order of magnitude smaller. With solution times increasing at least by a power of three with reduction of element size, current available computing power does not seem adequate to carry out detailed 3D finite element analysis of the hard turning process.

The second group of (hard) turning models work in the tool reference plane (or parallel to it). These models are mainly aimed at predicting surface properties. In Section 2.1.3 Brammerz's theory [10] has already been examined, which essentially is a model for the achievable surface roughness in turning processes.

Both Jochmann [21] and Kelly [42] use numerical approaches to simulate the surface roughness in the tool reference plane. By including a history of tool positions in their models they are able to extrude the two dimensional model into a real surface. It also allows them to include spindle error motions (Jochmann) and specific cutting force variations (Kelly) in their models. The effect of either is a modification of the relative position between tool and work piece which impacts on the surface topography.

A specialist model for describing the development of white layers and thermal effects in hard turning is given in [43]. This model uses a moving heat source and a temperature history to assess metallurgical changes in the newly hard turned surface. By correlating tool wear (wear mark width V_B) with heat input into the work piece a relationship between tool wear and white layer generation is established.

2.2 "Ultra-precision" turning machines

The term ultra-precision machining is defined by Taniguchi as "those processes/machines by which the highest possible dimensional accuracy is ... achieved at a given point in time" [44]. That was in 1983. He went on to say that "Today [in 1983] ultra-precision machining means the achievement of dimensional tolerances in the order of 0.01µm ... and surface roughness of 0.001µm (1nm)."

In contrast to this surfaces of optical quality start at roughness of R_a=10nm, although of course there are many optical applications where better surface finishes are required. Despite the fact that colloquially machining of surfaces with optical quality is often equated with ultra-precision machining, using Taniguchi's definition this is not necessarily the case. From the predicted development today's ultra-precision machine tools should be capable of machining to accuracies of better than 1nm. Consequently roughnesses should be in the order of 0.1nm. While there are machines and processes that can potentially work to these accuracies they have no practical relevance in the machining of hard steels.

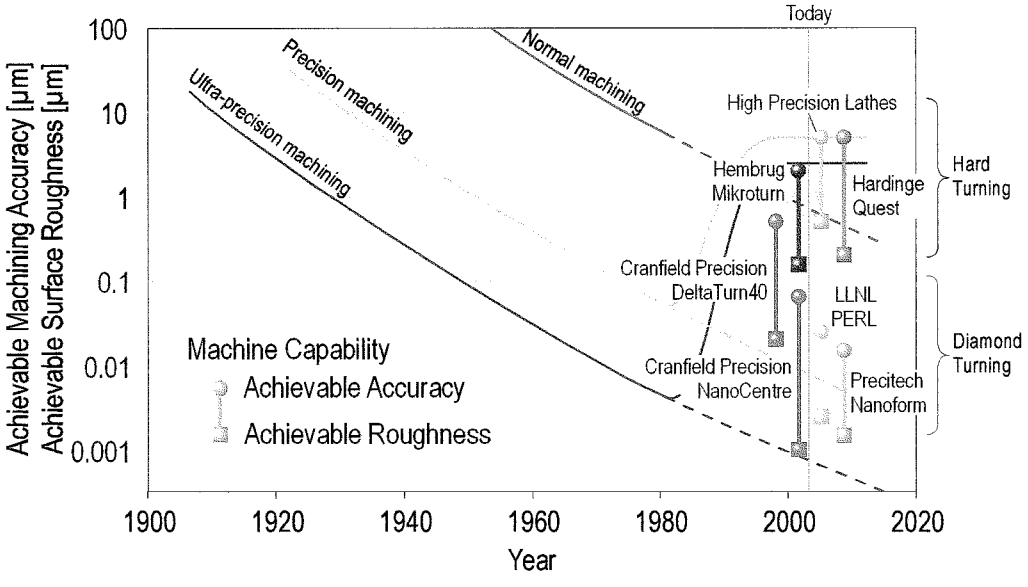

Figure 11: Development of machining accuracy after Taniguchi in comparison to current turning machines

Figure 11 shows Taniguchi's diagram predicting the development of machining accuracies. After 1980 the extrapolated developments are shown as dashed lines. In contrast a selection of current lathes have been examined for their capability in terms of achievable accuracy and surface roughness[3]. Probably for marketing reasons a large number of lathes today are referred to as precision lathes, despite the fact that they are quite common machines. According to Taniguchi these lathes today should achieve accuracies that are well sub-micron. In fact most will probably only achieve 5-10µm. To differentiate between these 'precision' lathes machines that are more precise are now referred to as "ultra-precision" or "super-precision" in the case of the Hardinge Quest, despite the fact their achievable accuracies are several orders of magnitude higher than defined by Taniguchi.

There seems to be a group of "ultra-precision" lathes, which in their application are close to normal manufacturing and aim to replace production grinding. These lathes are capable of hard turning. In fact the data plotted in Figure 11 is primarily from hard turning tests. These lathes start at machining accuracies of 5µm and achievable roughnesses of R_a 0.2µm and range down to accuracies and roughnesses approximately an order of magnitude better. The machines reviewed here in this range are the Hardinge Quest, the Hembrug Mikroturn50 and the Cranfield Precision DeltaTurn40.

The achievable accuracies of this group of machines reduces in line with the introduction of 'ultra-precision technology'. The Harding Quest lathe is of conventional design using rolling element slides and spindles, but has a polymer concrete base.

In contrast both the Mikroturn50 and the DeltaTurn40 are fully hydrostatic machines and employ positioning systems with higher resolution. The DeltaTurn40 is described in more detail in 4.1.

[3] For some lathes there is incomplete data in the public domain as far as achievable accuracy and surface roughness is concerned. If in doubt the assumption has been made that the achievable roughness is approximately ten times smaller than the achievable accuracy. The diagram should therefore is only used to illustrate the nomenclature of current machine tools, but does not allow an accurate assessment of relative performance.

For reference a number of dedicated diamond turning machines are also included in Figure 11. These machines, namely the Cranfield Precision Nanocentre, the LLNL PERL and the Precitech Nanoform200 operate on an all together different level of both accuracy and surface roughness than the ultra-precision hard turning machines. It must be pointed out that the accuracies for these machines is typically quoted in form accuracy rather than size which is due to the fact that these are predominantly used for the manufacture of optical components and makes a comparison with the hard turning machines more difficult. The quoted accuracies and roughnesses for these machines are about an order of magnitude better again than for the hard turning machines.

Despite the increased accuracy by Taniguchi's standards these machines only just qualify for 'precision machine' status. In fact it is doubtful whether with this absolute definition of the term 'ultra-precision' there are any machines that satisfy the accuracy requirements and at the same time use a chip removal technique for the shaping of work pieces.

However if one uses the more general definition for ultra-precision of highest possible dimensional accuracy then both the hard turning machines and the diamond turning machines can be referred to as ultra-precision machines, provided it is understood that the term ultra-precision hard turning refers to a different accuracy than the ultra-precision diamond machining or ultra-precision grinding.

2.3 Competing processes

Processes competing with ultra-precision hard turning can be grouped broadly into two categories, namely:

- Ultra-precision cutting processes
- Ultra-precision abrasive processes

As far as *ultra-precision cutting processes* are concerned there are not many alternatives to hard turning. This is not so much due to a lack of machine tools as to a lack of a suitable cutting material. Ultra-precision cutting processes in other materials, namely copper and aluminium, are carried out with monocrystalline diamond tools. The difficulty in machining steel with diamond is the high solubility of carbon in iron, which normally leads to excessive tool wear. There are attempts however to resolve the problems associated with high diamond wear when cutting ferrous metals.

Attempts to reduce chemical interactions between diamond and the work piece material are described in [45]. It was found that the exclusion of oxygen from the cutting zone did not yield an improvement in tool life. However some progress was made with cooling the cutting zone to cryogenic temperatures with help of a liquid nitrogen jet. The cryogenic cutting doubled the diamond tool life to a cutting distance of 200m. This is still only a fraction of what a CBN cutting tool would normally last (>4000m).

Some work has also been carried out into modifying the diamond as a cutting material [46]. The effect of coatings and implantation of chromium ions is reported. However only a TiN coating seemed to improve tool wear by about 50% in comparison to the untreated diamond.

The most promising method for increasing diamond tool life seems to be vibration cutting [47], [48], [49]. In this research a high-frequency linear or elliptical vibration is superimposed on the conventional feed motion of the cutting tool. Initial experiments were carried out in soft stainless steel, later hard steel was machined. In both cases an increase tool life of an order of magnitude was observed, bringing the cutting distance to the lower limit of what is expected of CBN tools. At the same time the surface roughnesses achieved were of optical or near optical quality. The main disadvantage of this technique is the very low cutting speed which is typically v_c=2.5m/min. In comparison to CBN cutting speed of v_c=100-240m/min this would lead to very low productivity. There may be cases where the advantages of this technology outweigh the productivity issues, but for the manufacture of most high precision work pieces this will not be acceptable.

In summary there are interesting developments in the cutting of steel with diamond cutting tools, but at this moment in time these are unlikely to have any significant impact on industrial manufacturing.

Abrasive processes which compete with ultra-precision hard turning are normally high- and ultra-precision grinding processes. Despite the fact that there are other abrasive processes capable of generating very high quality surfaces, these are not normally suited to generating and controlling the macroscopic shape of a work piece. This however is a key feature of hard turning and grinding.

Ultra-precision grinding processes can currently offer very low surface roughnesses ($R_a < 5$ nm) [50], [51]. The described grinding processes are planar surface grinding processes using cup-wheels. Electrolytic in-process dressing (ELID) can be used to maintain good grinding conditions throughout the cuts, however the better roughnesses are achieved without ELID.

It is argued that the kinematics of the cup-wheel grinding process are particularly suited to achieving surfaces of high quality on components where there is conformance between a long section of the grinding wheel arc and the work piece surface. The simplest (but not the only) case of this is the grinding of a flat work piece with a flat profiled cup wheel.

The explanation for the good surface roughnesses is that the leading edge of the grinding wheel carries out most of the cutting action in a primary material removal zone. In contrast the annular flat region of the grinding wheel trailing the primary removal zone carries out a finishing operation by repeatedly passing a large number of grinding grits over the machined surface. This leads to a considerable improvement in surface roughness compared to grinding processes where this finishing does not take place (e.g. plunge grinding). The finishing is more effective the larger the contact area between grinding wheel and work piece. This explains why the conformance of grinding wheel and work piece is of importance.

Ultra-precision grinding processes like this are in use in the grinding of semi-conductor and optical materials. [52], [53], [54]

It is of course possible to achieve ultra-precision machining results by combining several machining processes. In this case a semi-finishing process is used to shape a component and bring it as close as economically viable to the finished size plus any extra stock that may be required for the final finishing. These semi finishing processes for hard steel can be hard turning, grinding or any other process capable of machining hard steel. The process choice depends on the specific requirements of a particular component.

A wide range of finishing processes with varying characteristics exist which are potentially suited as a finishing processes. The main aim of the finishing process is to produce the desired surface topography in terms of roughness, waviness and material ratio, but also has to deliver the right surface integrity such as residual stress magnitude and profile.

An in depth discussion of the available finishing processes would extend well beyond the remit of this literature review. A selection of finishing processes and some key characteristics is given in Table 2 below.

Process	Mechanism	Achievable roughness	Comment
Roller burnishing	Plastic deformation	½ of previous R_a	Generates high compressive stresses
Shot peening	Plastic deformation	Not used to improve roughness	Generates high compressive stresses
Superfinishing	Chip removal with fixed abrasive	R_a>0.01µm	
Lapping	Chip removal with loose abrasive	R_a>0.01µm	Mainly used for flat surfaces

Table 2: Selected finishing processes used after hard turning

3 SCOPE OF WORK

From the literature review in the previous chapter it is clear that hard turning on ultra-precision machine tools is not wide spread with average roughnesses achieved so far in the range of several tens of nanometres. In that respect the development of a hard turning process capable of delivering surface roughnesses of single-digit nanometres would be a significant improvement on existing technology and is the fundamental aim of this work. In order to achieve this target a better understanding has to be gained on how the surfaces in hard turning are generated. Current cutting theory must be reviewed and compared with experimental results to tests its validity for ultra-precision hard turning.

From existing knowledge and experimental results an accurate method of predicting achievable roughness should be derived. This needs to take into account the relevant factors and cutting parameters. Where possible this should be done in a way that reflects the underlying mechanism. Failing that, the experimental data created during the course of the work could he used to create look-up tables – where necessary with interpolated values.

The roughness prediction should be robust enough to include tool wear. As it is known that roughness in hard turning can be strongly affected by wear it is necessary to make provisions for that. A particular understanding of how tool wear affects roughness should be gained during the course of the work. The insights into tool wear should then be used to modify and refine the surface roughness prediction.

4 EQUIPMENT & PROCEDURES

4.1 The DeltaTurn40 ultra-precision lathe

A precision chucking lathe, the DeltaTurn40 has a unique 'minimised machine-loop' design to yield component accuracy higher than can be achieved on machines of conventional design. Configured as a fully automated production cell, the machine utilises unique machine tool technology to overcome errors inherent in most machine tools. Thus it is possible to ensure a reliable process capability of sub-micron geometric accuracies [55], [56].

To achieve the combined accuracy and productivity demonstrated by the DeltaTurn40, three crucial factors are combined:

- Optimum mechanical design, where the focus is on static and (more importantly) dynamic stiffness, minimised thermal sensitivity, and precise motion. In addition, it is important that performance is maintained throughout the life of the machine.
- Control over the non-machine variables introduced by the machining process (e.g. tool wear) and by the environment (e.g. thermal drifts), through monitoring and feedback of machined-component parameters.
- High performance CNC and servo technology to control the relative positions of the component and tool.

The DeltaTurn40 machine has been designed with the work zone volume specifically restricted to machining components within 50mm length and 70mm diameter. This permits the application of technology that cannot be applied as effectively to a machine with larger axis strokes.

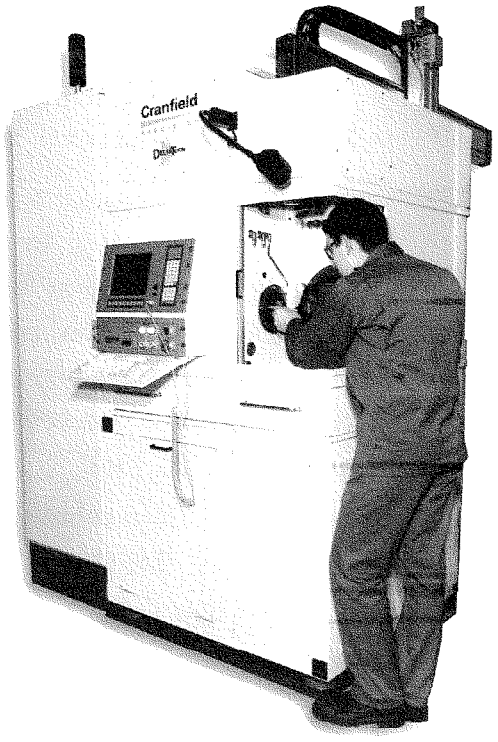

Figure 12: The DeltaTurn40 ultra-precision lathe

Critical to the performance of the DeltaTurn40 is the application of a non-contact 2-axis scanning head and single plate grating scale. The scale is mounted in the plane of the cutting tool and work spindle axis, with the minimum of offsets in X and Z directions to reduce Abbe errors[57]. The chosen configuration removes both the base structure and the guideway bearings from the overall machine loop stiffness; it also radically reduces the machine's thermal sensitivity. In the past such advantages have come only by using laser interferometry, but of course with the penalty of high cost.

Another advantage from this use of the 2-axis scale is that orthogonality between the machine axes motions is determined by the orthogonality between lines on the grating rather than from the machine base or alignment of guideways. Geometry is therefore constant, unaffected by thermal or other physical changes in the base structure, or by carriage bearing alignment. This ensures that the correction profiles for scale orthogonality error (determined on the machine during build) will remain correct.

Hydrostatic linear bearings have been selected for their almost frictionless motion with high damping and their enduring precision. The work-spindle bearing is also hydrostatic, with a design to maximise stiffness.

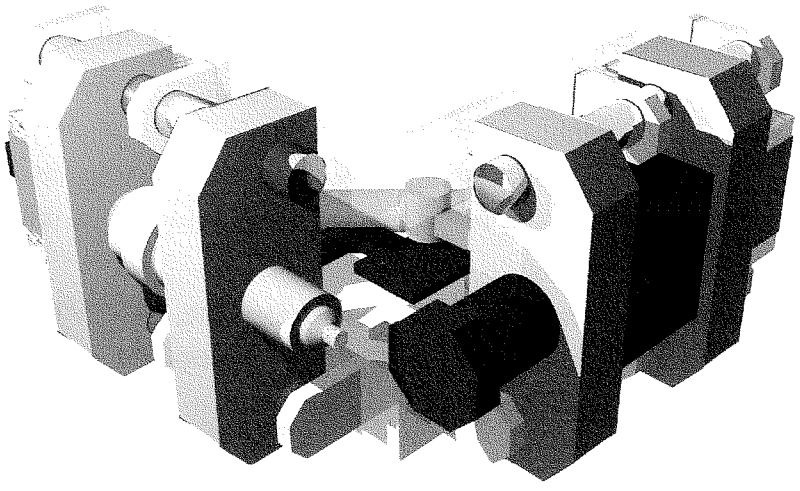

Figure 13: Schematics of the DeltaTurn40

The machine base structure is of space frame construction in a triangulated format (hence the "Delta" in DeltaTurn40), optimised for stiffness using finite element analysis techniques, internally damped and vibration isolated from the outer machine structure.

Finally, errors from temperature fluctuation in coolant and hydrostatic oil and spindle growth are reduced by careful application of separate closed loop temperature control systems, integrated with the machine control system.

Voice coil devices, mounted in direct line with work piece and tool centrelines, with closed loop position control utilising the latest state of the art DSP technology drive the linear axes. Drive stiffness, especially dynamic stiffness, and positioning capability do not suffer from the de-coupling effects typically found in ball-screw drives. The carriage mass of each axis has been minimised for best performance.

4.2 Sample work pieces

As stated previously one of the aims of this work was to develop a cutting process for finish machining of surfaces on a continuously variable transmission (CVT) shaft. This component and its outline dimensions are shown in Figure 14. The surfaces requiring ultra-precision machining are highlighted in the drawing.

With a work volume of ∅70×50mm on the DeltaTurn40 clearly a smaller scale component was needed for process development purposes.

For the test work pieces bar stock was parted off to form work pieces ∅42×70mm long. These were then through hardened to HRc 62±2. Although the real CVT component is induction hardened, the through hardening process for the sample components was the only option available at the time. One advantage of the through hardening is that the sample work pieces can be re-cut several times while still maintaining the desired hardness.

The material specification for both the CVT component and the sample work pieces was 51CrV4. The measured material composition is given in Table 3.

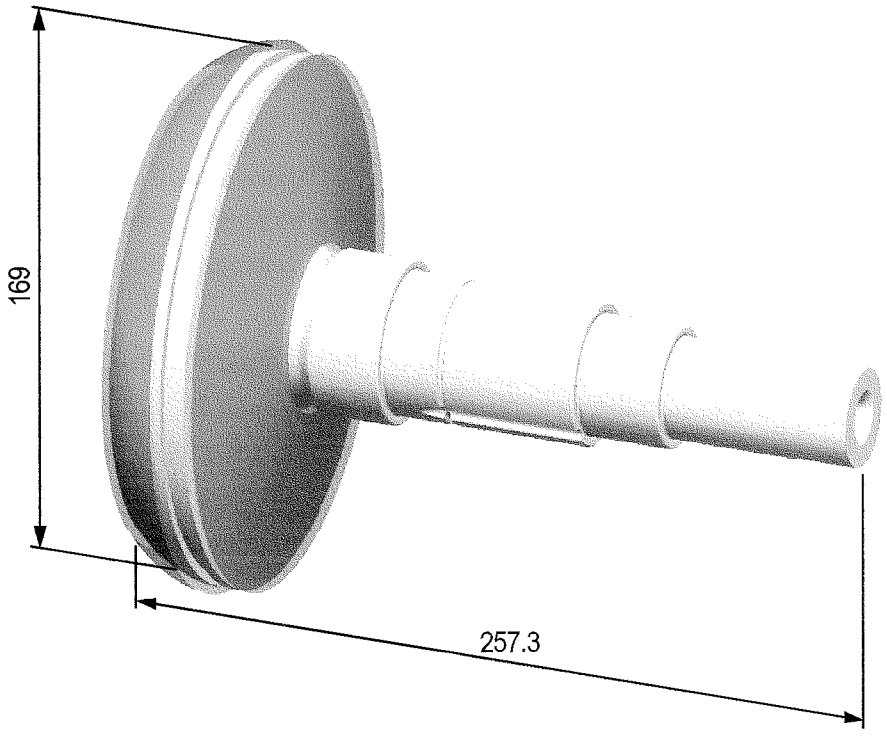

Figure 14: CVT component, ultra-precision machined surfaces indicated in red

Element	Specification [%]	Measured [%]
C	0.46 - 0.54	0.53
Mn	0.60 - 0.90	0.81
P	< 0.035	0.015
S	< 0.04	0.007
Si	0.15 - 0.35	0.19
Cu	- - -	0.15
Ni	- - -	0.06
Cr	0.80-1.15	0.95
V	> 0.15	0.25

Table 3: Material Composition of the CVT work piece (51CrV4)

Figure 16 shows the hardness profile of the sample work pieces (data recorded from three randomly selected samples). The microhardness profile (HV) shows a thin relatively soft skin (ca. 560HV) on the outside of the work piece. Within less than 0.5mm from the surface the hardness stabilises around an average of 650-700HV, although recorded values range down to 600HV in places. The inner section of the work piece radius shows slightly softer material in the range of 600-650HV. A small central core of higher hardness can also be seen. This hardness profile roughly corresponds to the appearance of the surface after preparation for detailed metallurgical analysis (Figure 17).

Confirmation measurements with a standard workshop Rockwell hardness tester show hardnesses of approximately 2HRc higher than recorded with the Vickers microhardness tester. This can be explained with metrology and scale conversion errors and is within the expected variability.

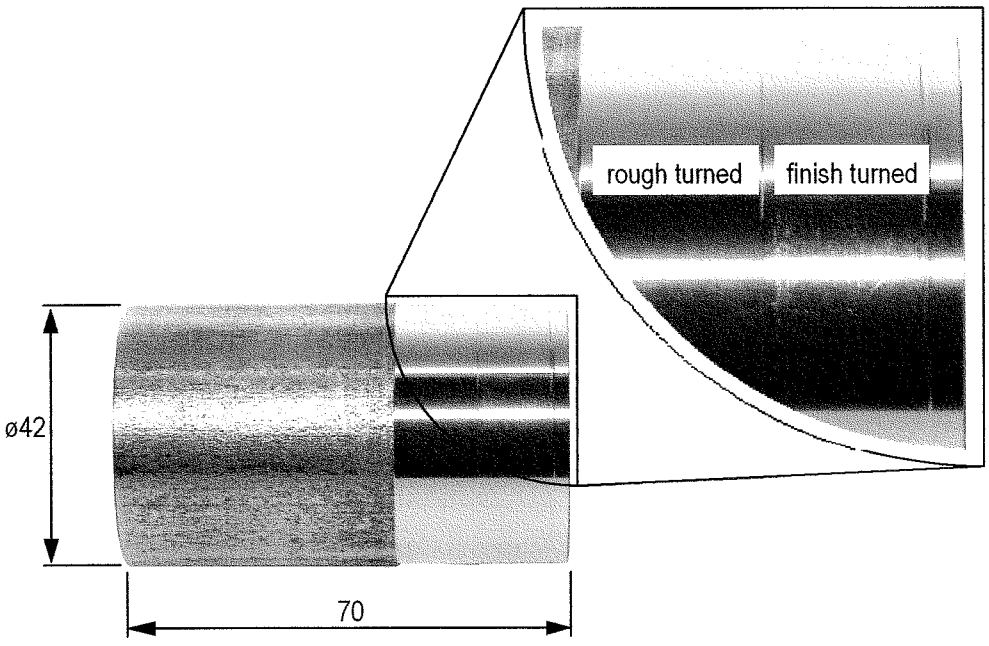

Figure 15: Hard Turning development component

The component shown in Figure 15 highlights one of the difficulties in assessing hard turned surfaces visually. The rough turned surface, which was machined with a much higher feed rate than the finish turned surface, to the naked eye appears more pleasing. This is due to the fact that surfaces in a range from approximately R_a 300µm to R_a 600µm surfaces have a very uniform – albeit slightly dull – appearance. Those surfaces on the other hand which have been created with low feed rates and very low surface roughness appear highly reflective, but also exhibit banding due to diffraction effects. In addition any other surface irregularities, whether they are due to defects in the work piece material, the cutting process or post-process contamination, can be seen very clearly against the backdrop of this reflective surface.

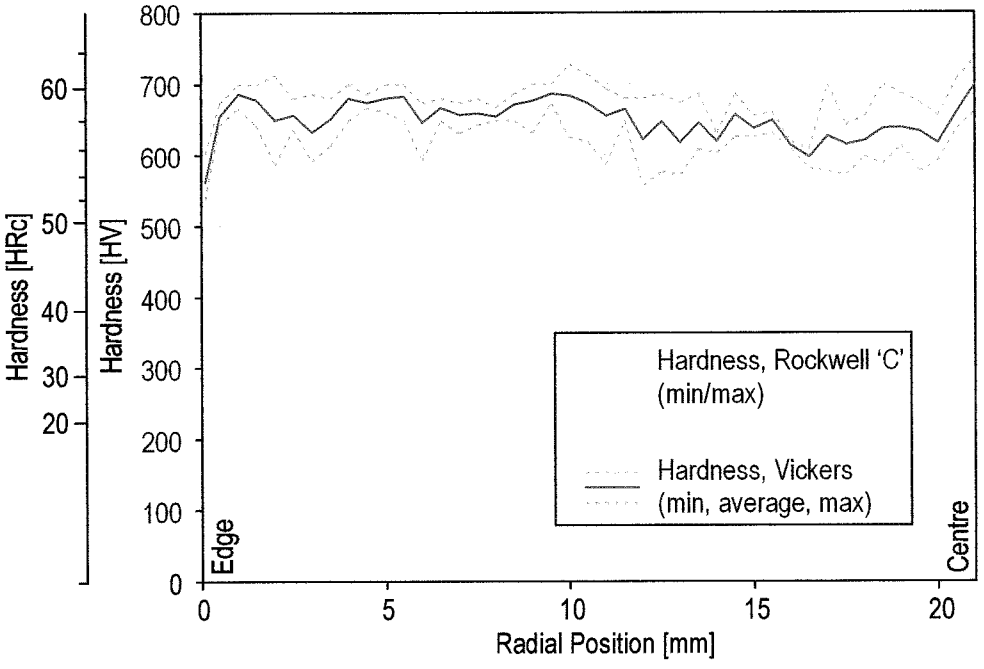

Figure 16: Hardness profile of sample work pieces

Samples for metallurgical analysis were prepared by sectioning the test pieces at 6mm and 35mm distance from one of the end face. The sections were then ground and polished according to Table 4. Finally an etching process (Vilella's reagent 50%, 8 s) prepared the surface for microscopic assessment.

Step No.	Process	Medium	Parameters	Time
1	Grind	Al_2O_3 grinding wheel (surface grinder)		Until flat
2	Grind	SiC 220grit grinding pad	150 rpm 50lbf	120min
3	Grind	SiC 1200grit grinding pad	150 rpm 50lbf	120min
4	Polish	MD Allegro Resin Pad + liquid diamond 9µm water miscible	150 rpm 50lbf	10min
5	Polish	DP Pan + liquid diamond 6µm water miscible	150rpm 50lbf	5-10min
6	Polish	DP Dur + liquid diamond 3µm water miscible	150rpm 50lbf	5-10min
7	Polish	Polishing cloth + masterpolish suspension (silica)	60rpm 25lbf	2min

Table 4: Typical sample preparation for metallurgical analysis.

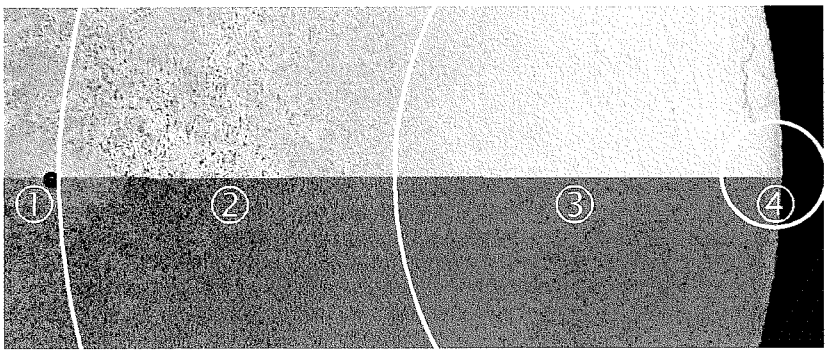

Figure 17: Etched sample surface (visual light and false colour image)

4.3 Metrology

Surface roughness measurements were mainly carried out with a Taylor Hobson Form Talysurf. The Talysurf uses a contacting probe with a stylus radius of 2µm. The actual measurement of the stylus displacement is done by laser interferometer.

For measurements conforming with the relevant ISO and BS standards the following parameters were used:

Measuring length	4 mm
Cut-off length	0.25mm or 0.08mm
Number of Cut-offs	16
Roughness Filter	Gaussian
Probe resolution (with 60mm length stylus)	10nm
Output after internal processing with the Talysurf software:	
Resolution of interpolated output height data	0.001nm
Sample Spacing (along work piece surface)	0.25µm

Table 5: Surface roughness measurement parameters (Talysurf)

While the Talysurf is quick and convenient to use for most surface roughness measurements there has to be some doubt on its accuracy when measuring very low surface roughnesses. Both the sample spacing and the stylus radius may lead to inaccurate results, which need to be verified with other more accurate measurements.

In some cases it was desirable to use non-standard settings for the surface roughness evaluation. In those cases the unfiltered data was exported from the Form Talysurf and processed in a mathematical software package.

Typically a short measuring length was extracted from the data (in the order of $10\times f$). This data was then levelled by fitting and subtracting a third order polynomial. The surface roughness parameters (R_a, R_t) were then calculated from the data treated as a single cut-off according to Equation 1 and Equation 3. This technique tends to give lower figures for both R_a and R_t than the standard evaluation and is therefore limited in its usefulness for production purposes. On the other hand it allows the isolation of the kinematic roughness from lower frequency tool or machine oscillations. Once the kinematic roughness has been isolated it allows a better assessment of what is happening in terms of surface generation from one revolution of the work piece to the next. In subsequent chapters it is made clear in the context of given surface roughness measurements which assessment length was used.

Surface roughness has also been assessed with a Wyko RST interferometer. The Wyko measured surface roughness in an area of approximately 250×250µm. It is particularly suited to the measurement of very low surface roughnesses (R_a 0.02 and below). The Wyko was predominately used as a way of confirming the measuring accuracy of the Form Talysurf. In measurements so far the difference in R_a measured on the same work piece and in approximately the same area are in the order of 2-4nm.

Measuring Area	105×117µm^2
Instrument resolution	10nm
Repeatability (R_q)	3nm
Resolution of interpolated output height data	0.001nm
Spatial Sampling Limit	0.48µm

Table 6: Surface roughness measurement parameters (Wyko RST)

Related to the work piece surface roughness measurements is the measurement of tool profile and cutting edge roughness. The tool profile and roughness measurements were carried out on the Form Talysurf. The strong curvatures on the tool surfaces do not allow the use of the Wyko RST interferometer.

When recording the tool profile there are two primary profiles, which need to be considered (see Figure 18). One profile is recorded along the cutting edge and gives a measure of tool corner radius and the roughness that the work piece is exposed to (tool reference plane). The second trace is taken on a plane perpendicular to the cutting edge and should pass through the centre of the contact zone between cutting tool and work piece (tool back plane). This trace is needed to assess the angles between tool faces and flank. It also allows the assessment of the cutting edge radius.

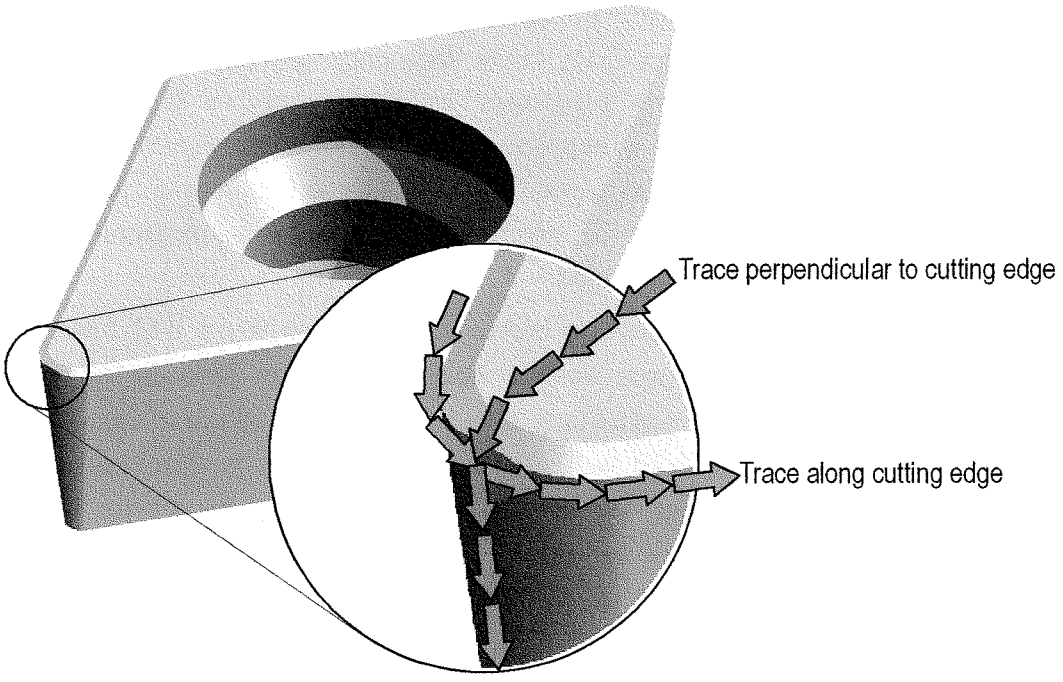

Figure 18: Primary tool profiles

The difficulty in measuring traces off the cutting tool (in particular along the cutting edge) is registering a particular location on the cutting edge to that part of the work piece that has been created by it. An in situ measurement of the cutting edge on the machine does not seem feasible, therefore these measurements have to be carried out away from the machine tool. Even if the cutting tool is mounted in a repeatable tool holder it still proves very difficult to register the traces along the cutting edge to the work piece surface. This is probably due to repeatability of the tool holder location during the transfer of the tool holder from the Form Talysurf to the machine tool. Further difficulties in registration of the profiles are caused by attempting to match a convex profile (i.e. the cutting tool) to a concave profile (i.e. the surface roughness), both of which are affected in different ways by the stylus radius.

In order to overcome this problem a different method of determining the profile along the cutting edge was employed. From [58], [36] it is known that the cutting edge profile is replicated with good quality in the machined surface. It is possible to exploit this effect to obtain a cutting tool profile for the precise part of the cutting tool, which has generated a particular region of the surface. When generating profile data in this way care has to be taken that effects of the minimum undeformed chip thickness do not distort the recorded profile.

By using a specifically designed work piece and cutting sequence (shown in Figure 19) it is possible to leave a suitably wide imprint of the tool profile in the work piece surface prior to machining at low feed rate.

The work piece has a short section at the start of the machining zone, which is machined with the same cutting tool that will also generate the surface at low feed. Only a small number of work piece revolutions are required for this initial section of the work piece. Typically feed rates of f=150µm and 200µm were used for this section. These large feeds gave sufficiently wide areas in the bottom of each groove to assess the tool profile even if minimum undeformed chip thickness effects occurred.

The area of low feed, which is used for the assessment of the surface roughness is separated by a groove ca. 300µm deep from the high feed area. In this way the transition from high feed to low feed is clearly visible in any surface roughness trace. The groove is machined into the work piece with a roughing tool.

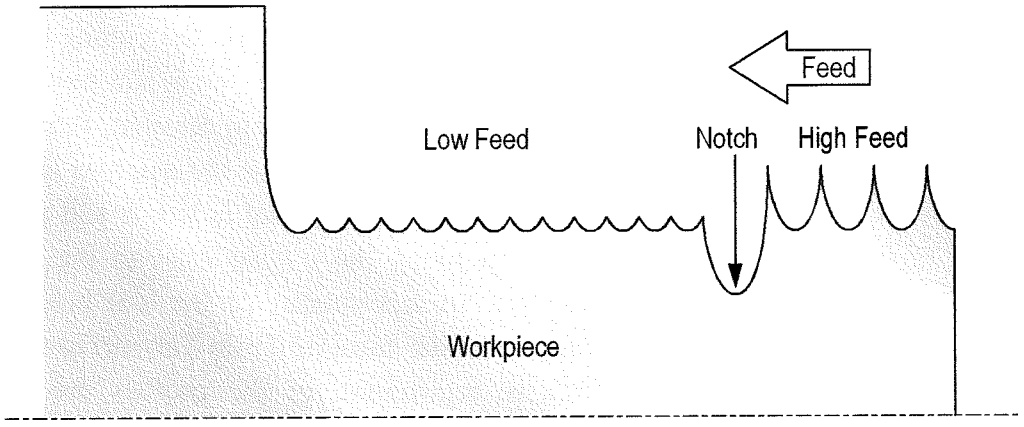

Figure 19: Sample work piece for recording the tool profile prior to low-feed machining

Once on the Form Talysurf the entire work piece surface is measured in a single long trace. This part of the trace can later be selected for surface roughness analysis on the Form Talysurf itself or the data can be exported and analysed elsewhere.

Hardness measurements were carried out with a micro-hardness tester according to Vickers and a standard workshop hardness tester after Rockwell.